Second-order overtone and combination modes in the LOLA region of acid treated double-walled carbon nanotubes

A. V. Ellis
Industrial Research Ltd., Nanotechnology Platform, P.O. Box 31310, Lower Hutt, New Zealand

(Received 31 March 2006; accepted 16 August 2006; published online 28 September 2006)

Moderate acid treatment of double-walled carbon nanotubes (DWCNTs) has given rise to two new experimentally observed second-order double resonant Raman scattering frequencies centered at 1901 cm^{-1} and 1942 cm^{-1}, in the highly dispersive LOLA region. These LOLA overtones and combination modes have been predicted by double resonance theory for two phonons associated with the *K*- and Γ-points, respectively. © *2006 American Institute of Physics*.
[DOI: 10.1063/1.2354081]

In their pristine state carbon nanotubes are insoluble in water making them incompatible with the water-based environment of living systems. Recent evidence has shown that water-dispersible, in particular, side-walled functionalized carbon nanotubes are substantially less cytotoxic to humans than surfactant stabilized pristine nanotubes.[1,2] This means that more than ever the effects of side-wall functionalization on these formulated "green" nanotubes needs to be studied. More important is the study of the impact that side-wall modification plays on the electronic properties of carbon nanotubes particularly if they are to be used in future applications, such as, nanotube doped conductive polymer nanocomposites,[3–5] biosensors, actuators and molecular electronics.[6–8]

One of the most common and facile techniques for rendering carbon nanotubes soluble is wet chemical oxidation. This can easily be achieved by ultra-sonication or reflux in concentrated HNO_3/H_2SO_4 (Ref. 9) which facilitates direct covalent sidewall functionalization at defect sites. The technique is known to introduce hydroxyl, carboxyl, carbonyl, and ether-type moieties[9] at the ends and sidewalls of nanotubes, in particular at localized Stone-Wale defects. Defect sites cause local changes in the density of states (DOS) in graphene layers.[10,11] It is therefore expected that any change in the DOS at the Fermi level of acid treated nanotubes, will change their electronic and vibrational properties. Such changes in the DOS may arise from the creation of sp^3 pendant bonds, the oxidation of pendant bonds,[12] the introduction of heptagon-pentagon rings and the doping of the sp^2 graphene layers, for example by nitrogen or sulphate groups.[13]

A powerful and nondestructive method used to determine the vibrational modes of graphitic nanostructures is Raman spectroscopy.[14,15] It has also been proven useful in determining the diameter and chirality of single-walled carbon nanotubes (SWCNTs).[16] A number of publications have dealt with the phonon dispersion relation of 2D graphite,[17,18] and this has subsequently been applied to carbon nanotubes.[19] Typically, only zone-center Raman modes are observed, normally from the first-order spectra, as double-resonance Raman spectra do not provide the phonon dispersion relationship. This is because the wave vector in the first-order Raman scattering process is too small to create phonons from the incoming photon from such a large distance from the Γ-point. However, the second-order Raman scattering processes show that there are low-intensity features in the Raman spectra that do not come from the Γ-point. These peaks in the second-order Raman spectra can be classified as two-phonon peaks and disorder-induced one-phonon peaks. Reich and Thomsen[20] explained the dispersion of the *D*-band phonon frequency by a double-resonance process. This was then applied to all six branches of the phonon dispersion relations of graphite so that a number of disorder-induced peaks can be assigned as non-zone center phonon modes. The scattered intermediate states and final states are actual electronic states and this has allowed a more feasible analysis of defect interaction processes. This relation is very important in determining the origin of disorder, particularly when related to disorder that is induced in a controlled fashion as a step process in functionalization. It has been shown that the peak at D' (ca. 1620 cm^{-1}) is directly related to the induced disorder when more defects are created in nanotubes.[21] Here we look at the change in second-order Raman scattering modes of acid treated double-walled carbon nanotubes (DWCNTs), which are considered to be a coaxial combination of two SWCNTs, containing an inner (I) and an outer (O) tube. This combination can be semiconductor (I)-metal(O) or metal(I)-semiconductor(O).

Using Raman scattering we have identified experimentally, for the first time, two new second-order LOLA overtones and combination modes for two phonons associated with the *K*-point and the Γ-point according to double resonance theory.[22] The modes are centered at 1901 cm^{-1} and 1942 cm^{-1} for $E_{laser}=1.96$ eV. These new modes appear only after acid treatment and give an LOLA peak splitting of $\Delta\omega_{LOLA}=41$ cm^{-1}.

DWCNTs [NanoLab (MA, USA)] were treated with acid, following the method of Ellis and Bubendorfer.[23] Briefly, nanotubes were weakly sonicated at 60 W in concentrated sulphuric and nitric acid (7:3 vol/vol) for 2 h. The resulting suspension was filtered through Whatman filter paper (0.45 μm) and washed with de-ionized water until the

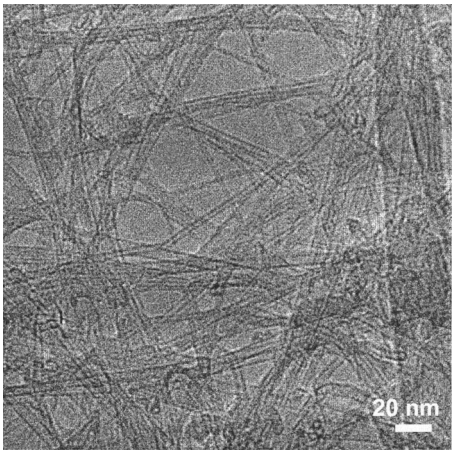

FIG. 1. Typical HRTEM of pristine and 2 h acid treated DWCNT sample.

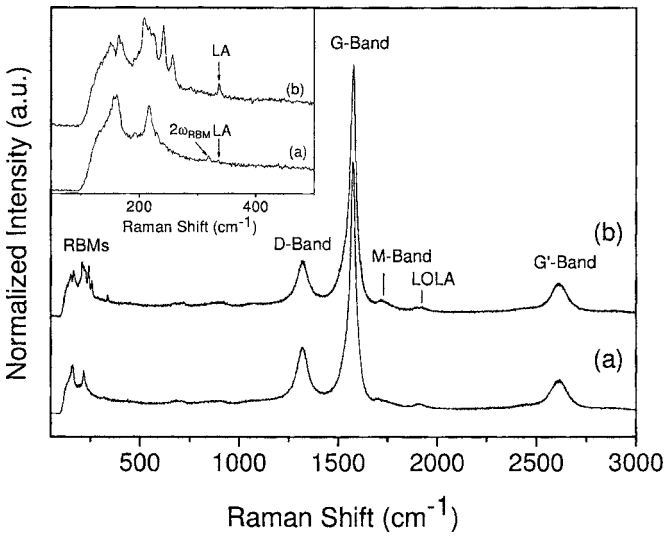

FIG. 2. Raman scattering spectra of (a) pristine and (b) acid treated DWCNTs for $E_{laser}=1.96$ eV. Inset: expanded low frequency radial breathing mode (RBM) region.

eluate was neutral to pH paper. DWCNTs before and after treatment were dispersed in a toluene medium and transferred to a carbon-coated Cu-grid for high-resolution transmission electron microscopy (HRTEM) measurements in a JEOL-2010 TEM operated at 200 kV. Raman scattering analysis was carried out by placing dried samples onto a glass slide and using microscope laser Raman spectroscopy with a Jobin Yvon-LabRam HR spectrometer. The laser excitation was 632.8 nm (1.96 eV) with a spectral resolution of 1.5 cm^{-1}.

Figure 1 shows a typical high resolution transmission electron micrograph (HRTEM) of the pristine DWCNT sample. There is little amorphous carbon or large catalyst particles in the pristine sample. The average diameter distribution determined from this and other images show coaxial structures, that is, 1.08 ± 0.01 nm for the inner (secondary) tubes and 2.17 ± 0.04 nm for the outer (primary) tubes. There is no significant difference in the images obtained for the acid treated nanotubes and as such have not been presented here.

Previously we have reported Raman scattering analysis of DWCNTs up to 1.5 h acid treatment.[23] Here we report different findings in the 2 h treated samples. Notably, after acid treatment the spectra show changes in (a) the distribution of the Raman breathing modes (RBMs); (b) the intensity and position of the *D*-band doublet; and more importantly (c) the previously unobserved splitting of the second-order highly dispersive LOLA combination mode.

With respect to the RBMs, Figs. 2(a) and 2(b) shows the first and second order Raman spectra collected over the broad phonon frequency range 100–3000 cm^{-1} at $E_{laser}=1.96$ eV for the pristine and acid treated DWCNTs respectively. The first-order spectra of DWCNTs in the RBM region is fairly complex and arises from the mixing of many different $(n,m;n',m')$ DWCNT constituents, where (n,m) denotes the outer tubes and (n',m') denotes inner tubes, as observed by Li *et al.*[24]

Figures 2(a) and 2(b) inset shows the expanded low frequency Raman spectra between 50–500 cm^{-1} for the pristine and acid treated DWCNTs, respectively. Using the local density approximation the nanotube diameter (d_t) was calculated as $d_t=A/\omega_r$ where $A=243$ cm^{-1} nm.[25] The results of which are tabulated in Table I. It should be noted that the diameters shown here are only the ones within the laser excitation window, larger diameter tubes are not observed but were observed in the HRTEM. The retention of a bi-modal distribution after acid treatment suggests little exfoliation of the coaxial tubes, in agreement with the HRTEM images. It is therefore expected that any change in the electronic and vibrational properties is from surface modification rather than the formation of amorphous graphitic or carbonaceous material.

From Table I the mean interlayer coupling between the graphene sheets in both the pristine and acid treated DWCNTs was calculated from the average largest diameter outer tube minus the average smallest diameter inner tube, divided by 2 (Table I). That is, the average coupling for pristine DWCNTS is 1.91−1.13=78; 78/2=0.39 nm and for acid treated is 1.61−0.95=66; 66/2=0.33 nm. For pristine material the mean interlayer coupling has previously been calculated to be ~0.36 nm,[26] 0.39 nm[23] or up to 0.40 nm.[27] Both the results for the pristine and acid treated material are comparable to the van der Waals interaction in {002} graphite with a spacing of 0.335 nm.[27] It is this interlayer distance

TABLE I. Radial breathing mode (RBM) frequencies (ω_r) and diameters (d_t) for the primary (outer) tube and secondary (inner) tube of the pristine and acid treated DWCNT samples.

	RBM frequencies ω_r (cm^{-1}) and diameter $(d_t)^a$ (nm) of outer tube	RBM frequencies ω_r (cm^{-1}) and diameter $(d_t)^a$ (nm) of inner tube
Pristine	127 (1.91)	216 (1.13)
	159 (1.53)	
Acid treated	151 (1.61)	208 (1.17)
	164 (1.48)	216 (1.13)
		225 (1.08)
		242 (1.00)
		256 (0.95)

[a]$d_t=A/\omega_r$, where $A=243$ cm^{-1} nm.[25]

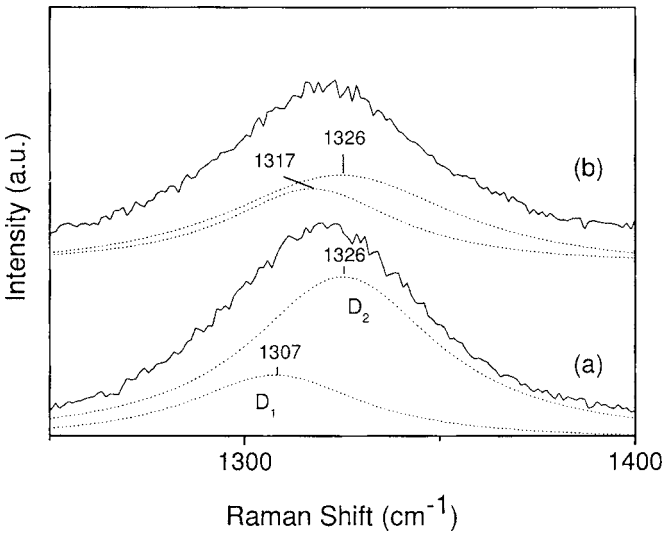

FIG. 3. Raman spectra of the D-mode at $E_{laser}=1.96$ eV. Solid lines show spectra of (a) pristine and (b) acid treated DWCNTs; the dashed lines are Lorentzian fits showing the D-mode doublet.

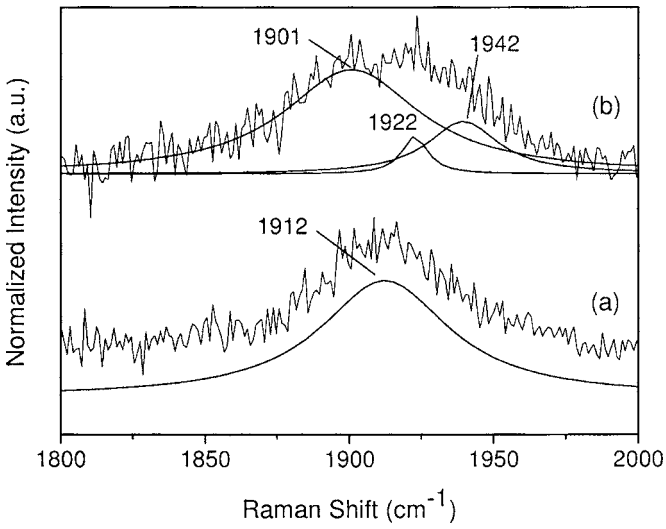

FIG. 4. Raman spectra of the highly dispersive LOLA (1900–1950 cm^{-1}) features at $E_{laser}=1.96$ eV. Solid lines show spectra of (a) pristine and (b) acid treated DWCNTs; the thin solid lines are Lorentzian fits.

that gives rise to the DWCNTs electronic stability. It appears that after acid treatment the interlayer coupling distance is reduced slightly.

For the pristine DWCNTs a weak second-order harmonic (overtone) feature is observed at 319 cm^{-1} (Fig. 2 inset). The features at 337 cm^{-1} observed in both the pristine and acid treated DWCNTs (marked with arrows) have been assigned to the resonantly excited dispersive acoustic LA (or L_2) mode in the longitudinal acoustic phonon branches observed in graphite whiskers at 335 cm^{-1}.[28]

In considering the D-band region (1300–1400 cm^{-1}) this is explained by an inter-valley double resonance mechanism that occurs around two nonequivalent K-points at neighboring corners of the Brillouin zone (BZ). In particular, this mode comes from the upper, fully symmetrical phonon branch, which is nondegenerate at the K-point.[29] This region is directly associated with amorphous and defect-induced disorder and here we describe how this has only slightly changed as a result of acid treatment.

Lorentzian line shape fitting of this region yields two peaks, assigned D_1 and D_2 (Fig. 3). These doublets arise from the two different time orders in the scattering process of the TO branch.[29] Figures 3(a) and 3(b) shows the D-band region for the pristine and acid treated nanotubes respectively. The lower energy shoulder D_1 is found at 1307 cm^{-1} in the pristine material and this is up-shifted by 10 cm^{-1} to 1317 cm^{-1} after acid treatment. The treatment may have resulted in a change in chirality and/or an increase in tube diameter of the bulk material. There is no apparent change in D_1 intensity.[27] The D_2 line is associated with lattice defects and finite length effects inherent in the nanotube structure. Its peak position and breath remain centered at 1326 cm^{-1} after acid treatment. However, the intensity does change and is reflected in the ratio of I_D/I_G, which decreases from 0.45 to 0.42 for the pristine and acid treated tubes, respectively. This suggests the removal of residual amorphous sp^2 carbon. The splitting of the D-band for the pristine material is $\Delta\omega=19$ cm^{-1} while after the acid treatment the splitting of the D-band reduces to $\Delta\omega=9$ cm^{-1}, as reported by Cançado *et al.*[30] The error in this estimate is ±1.5 cm^{-1}. Theoretically, this shift in graphene is expected to be $\delta\omega_D=E_{phonon}\times 50$ $cm^{-1}/eV=8.5$ cm^{-1}, where E_{phonon} is approximately 0.17 eV. Cançado *et al.*[30] explain that a split of this magnitude (9 cm^{-1}) in the Stokes spectra is associated with the scattering from a point around K to a point around K' by a phonon (D_1) or by a defect process (D_2). As only the D_1 peak shifts in this work then we expect that the inelastic phonon scattering process which connects points on the circles around K and K' with radii Δk_0 and $\Delta k_0-\delta q$, respectively, where δq is given by $\delta q=E_{phonon}/A$ and $A=\sqrt{3}\gamma_0 0.246/2$ has been changed due to acid treatment.

Most important are the new modes observed in the LOLA region. Brar *et al.*[31] have tentatively identified the higher frequency LOLA mode (or LO+LA mode) between 1850 cm^{-1} and 1950 cm^{-1} as a highly dispersive mode attributed to a second order combination of one phonon from the longitudinal optical branch (LO or D') plus one phonon from the longitudinal acoustic (LA or L_2) branch. Both of which can be explained by an intra-valley double resonance mechanism that occurs around the K-point in the Brillouin zone.[28]

Lorentzian line shape fitting of the LOLA region was used to determine peak positions. Figure 4(a) shows only one peak ω_{LOLA} at 1912 cm^{-1} (offset for clarity) for the pristine DWCNTs, providing evidence for the predictions of double resonance theory for $|q|\cong|2k|$ LO+LA combination modes, where q and k denotes the phonon and electron wave vector, respectively, measured from the Γ- and K-points. The peak observed here for DWCNTs is down-shifted by 14 cm^{-1} to that previously determined for SWCNTs (1926 cm^{-1} at $E_{laser}=1.96$ eV).[31]

The fulfillment of this double-resonance condition suggests that the sample contains symmetry-breaking elements such as boundaries at the crystallite surface. Alternatively the two-phonon scattering can be observed where momentum is conserved through phonons of equal but opposite wave vec-

tor. It is expected that there will be no observed double resonance feature related to $|q| \cong 0$ since $\omega_{\mathrm{LA}}=0$ and $\omega_{\mathrm{LO}}=\omega_{E2g}=1582\ \mathrm{cm}^{-1}$ for $|q| \cong 0$.

Significantly, after acid treatment Lorentzian curve fitting shows that the LOLA region exhibits three peaks [Fig. 4(b)]. A low frequency peak at 1901 cm^{-1}, a peak centered at 1922 cm^{-1} and a high frequency peak at 1942 cm^{-1}, $\Delta\omega=41\ \mathrm{cm}^{-1}$. The peak centered at 1922 cm^{-1} is attributed to the LO+LA mode, as described previously. The reason for its sharpness is unclear and would imply dispersionless behaviour similar to the dispersionless feature of the coalescence-induced mode (CIM) recently observed at approximately 1850 cm^{-1} by Endo *et al.*[32] and Fantini *et al.*[33] It is unclear why three modes are observed after acid treatment but may be due to defect-induced scattering or zone folding. The lower frequency at 1901 cm^{-1} is the predicted overtone and combination mode for a phonon associated with the *K*-point and the higher frequency at 1942 cm^{-1} is the predicted phonon close to the Γ-point and they fit well with the other possible predicted overtones and combinations modes according to double resonance theory.[22,31] This is the first time these modes have been observed experimentally for carbon nanotubes.

There is disagreement in literature regarding whether the peak observed between 1800–2000 cm^{-1} is due to the $\omega_G+2\omega_{\mathrm{RBM}}$;[34] or the iTOLA or the LOLA.[31] We believe it may be either the iTOLA or the LOLA mode depending on whether the tubes are pristine or defected. That is, the iTOLA mode for pristine nanotubes and LOLA for the acid treated nanotubes after defect formation.

In the case of the pristine material assuming the iTOLA combination mode=1912 cm^{-1} and the observed iTO mode =1574 cm^{-1} (Fig. 2). Then it follows iTOLA−iTO=LA. That is, $1912-1574=338\approx 337\ \mathrm{cm}^{-1}$. This is then true for the pristine material. Using $\omega_G+2\omega_{\mathrm{RBM}}$ for the pristine material, then $1574\ \mathrm{cm}^{-1}+319\ \mathrm{cm}^{-1}=1893\neq 1912\ \mathrm{cm}^{-1}$ so this explanation is not feasible.

For the case of the acid treated tubes. The iTOLA combination mode would be centered at 1922 cm^{-1} and the iTO mode is experimentally observed at 1574 cm^{-1} it stands then that iTOLA−iTO=LA. That is, 1922−1574=348 which does not equal the experimentally observed LA mode i.e., $\neq 337\ \mathrm{cm}^{-1}$. Therefore iTOLA does not relate to this mode. However, we take the LOLA to be centered at 1922 cm^{-1} and LA is observed at 337 cm^{-1}. It stands then that LOLA −LA=LO. That is, 1922−337 gives LO or (D') band $=1585\ \mathrm{cm}^{-1}$, this is not experimentally observed as the *G*-band is too broad but is a better fit for the data. In addition it is clear from literature that acid treatment causes defects, assigned to the D' mode.

Defect induced scattering may account for the frequency differences observed for the acid treated tubes, an effect due to phonon confinement similar to that observed in nanoparticles.[35]

It may be that for the acid treated DWCNTs the optical phonons (LO) are more sensitive to the interface properties. They appear to be confined to each layer and cannot propagate in the growth direction, a "phonon confinement length." Optical phonons in a layered structure, where there is no overlap, can be described by folding into the new mini zone boundary, π/d, where $d=d_1+d_2$ thickness of the layers of the graphene sheets similar to acoustic phonons.[35] It is important to note that this confinement effect for given materials may be different for phonons of different symmetries and as such the term confinement may have no physical significance.

In this letter we experimentally demonstrate new overtone and combination modes predicted according to double resonance theory. These modes are observed only after acid treatment of double-walled carbon nanotubes at $E_{\mathrm{laser}}=1.96$ eV. Further work will be continued on resonant Raman scattering to assign these peaks to higher E_{laser} values.

[1] C. M. Sayes, F. Liang, J. L. Hudson *et al.*, Toxicol. Lett. **161**, 135 (2006).
[2] R. H. Hurt, M. Monthioux, and A. Kane, Carbon **44**, 1028 (2006).
[3] B. McCarthy, J. N. Coleman, R. Czerw, A. B. Dalton, H. J. Byrne, D. Tekleab, P. Iyer, P. M. Ajayan, W. J. Blau, and D. L. Carroll, Nanotechnology **12**, 187 (2001).
[4] J. N. Coleman, S. Curran, A. B. Dalton, A. P. Davey, B. McCarthy, W. J. Blau, and R. C. Barkie, Phys. Rev. B **58**, R7492 (1998).
[5] S. Curran, D. S. Zhang, W. Wondmaqegn, A. Ellis, J. Cech, S. Roth, and D. Carroll, J. Mater. Res. **21**, 1071 (2006).
[6] S. S. Wong, E. Joselevich, A. T. Woolley, C. L. Cheung, and C. M. Lieber, Nature (London) **394**, 52(1998).
[7] M. S. Strano, C. A. Dyke, M. L. Usrey, P. W. Barone, M. J. Allen, H. Shan, C. Kittrell, R. H. Hauge, J. M. Tour, and R. E. Smalley, Science **301**, 1519 (2003).
[8] J. Kong, N. R. Franklin, C. H. Zhou, M. G. Chapline, S. Peng, K. Cho, and H. Dai, Science **287**, 622 (2000).
[9] S. A. Curran, A. V. Ellis, K. Vijayaraghavan, and P. M. Ajayan, J. Chem. Phys. **120**, 4886 (2004).
[10] T. Pietraß, J. L. Dewald, C. F. M. Clewett, D. Tierney, A. V. Ellis, S. Dias, A. Alvarado, L. Sandoval, S. Tai, and S. A. Curran, J. Nanosci. Nanotechnol. **6**, 135 (2006).
[11] A. V. Ellis and B. Ingham, J. Magn. Magn. Mater. **302**, 378 (2006).
[12] J. Chen, M. A. Hamon, H. Hui, Y. Chen, A. M. Rao, P. C. Eklund, and R. C. Haddon, Science **282**, 95 (1998).
[13] M. T. Martínez, M. A. Callejas, A. M. Benito *et al.* Nanotechnology **14** 691 (2003).
[14] M. S. Dresselhaus, G. Dresselhaus, A. Jorio, A. G. Souza Filho, and R. Saito, Carbon **40**, 2043 (2002).
[15] J. Kastner, T. Pichler, H. Kuzmany, S. Curran, W. Blau, D. N. Weldon, M. Delamesiere, S. Draper, and H. Zandbergen, Chem. Phys. Lett. **221**, 53 (1994).
[16] A. Jorio, A. G. Souza Filho, G. Dresselhaus *et al.*, Phys. Rev. B **65**, 155412 (2002).
[17] Y. Kawashima and G. Katagiri, Phys. Rev. B **52**, 10053 (1995).
[18] T. Livneh, T. L. Haslett, and M. Moskovits, Phys. Rev. B **66** 195110 (2002).
[19] Ge. G. Samsonidze, R. Saito, A. Jorio, A. G. Souza Filho, A. Gruneis, M. A. Pimenta, G. Dresselhaus, and M. S. Dresselhaus, Phys. Rev. Lett. **90**, 027403-1 (2003).
[20] S. Reich, C. Thomsen, G. S. Duesberg, and S. Roth, Phys. Rev. B **63**, 041401(R) (2001).
[21] A. G. Souza Filho, A. Jorio, Ge. G. Samsonidze, G. Dresselhaus, R. Saito, and M. S. Dresselhaus, Nanotechnology **14**, 1130 (2003).
[22] R. Saito, A. Jorio, A. G. Souza Filho, G. Dresselhaus, M. S. Dresselhaus, and M. A. Pimenta, Phys. Rev. Lett. **88**, 027401 (2002).
[23] A. V. Ellis and A. Bubendorfer, Chem. Phys. Lett. **412**, 449 (2005).
[24] F. Li, S.-G. Chou, W. Ren, J. A. Gardecki, A. K. Swan, M. S. Ürdü, B. B. Goldberg, H.-M. Cheng, and M. S. Dresselhaus, J. Mater. Res. **18**, 1251 (2003).
[25] J. Liu, A. G. Rinzler, H. Dai *et al.*, Science **280**, 1253 (1998).
[26] S. Bandow, M. Takizawa, K. Hirahara, M. Yudasaka, and S. Iijima, Chem. Phys. Lett. **337**, 48 (2001).
[27] P. Tan, S. Dimovski, and Y. Gogotsi, Philos. Trans. R. Soc. London, Ser. A **362**, 2289 (2004).

[28] P. Tan, C. Y. Hu, J. Dong, W. Shen, and B. Zhang, Phys. Rev. B **64**, 214301 (2001).
[29] J. Maultzsch, S. Reich, and C. Thomsen, Phys. Rev. B **70**, 155403 (2004).
[30] L. G. Cançado, M. A. Pimenta, R. Saito, A. Jorio, L. O. Ladeira, A. Griieneis, A. G. Souza-Filho, G. Dresselhaus, and M. S. Dresselhaus, Phys. Rev. B **66**, 035415 (2002).
[31] V. W. Brar, Ge. G. Samopnidze, M. S. Dresselhaus, G. Dresselhaus, R. Saito, A. K. Swan, M. S. Ünlü, B. B. Goldberg, A. G. Souza Filho, and A. Jorio, Phys. Rev. B **66**, 155418 (2002).
[32] M. Endo, Y. A. Kim, T. Hayashi, H. Muramatsu, M. Terrones, R. Saito, F. Villalpando-Paez, S. G. Chou, and M. S. Dresselhaus, Small **2**, 1031 (2006).
[33] C. Fantini, E. Cruz, M. Terrones, H. Terrones *et al.*, Phys. Rev. B **73**, 193408 (2006).
[34] S. D. M. Brown, P. Corio, A. Marucci, M. A. Pimenta, M. S. Dresselhaus, and G. Dresselhaus, Phys. Rev. B **61**, 7734 (2000).
[35] A. K. Arora, M. Rajalakshmi, and T. R. Ravindran, in *Phonon Confinement in Nanostructured Materials*, edited by H. S. Nalwa (American Scientific Publishers, Stevenson Ranch, 2003), Encyclopedia of Nanoscience and Nanotechnology, Vol. X, pp 1–13.